EFFECT OF BUILD ORIENTATION ANGLE ON MECHANICAL PROPERTIES AND FRACTURE BEHAVIOUR OF FDM 3D PRINTED PLA

Harikrishnan Krishnan Muraleedharan[1], Anandhu Aravind[1], Vishnu Vijayan[1], Jaymin Vrajlal Sanchaniya[2]
[1]Riga Technical University, Latvia; [2]Kaunas University of Technology, Lithuania
jaymin.sanchaniya@ktu.lt

Abstract. A fundamental process parameter that is underutilised in fused deposition modelling (FDM), but defines the geometry of the deposition of individual layers and therefore the mechanical behaviour of printed parts, is the build orientation angle. This article explores the influence of seven angles of building orientation (0°, 15°, 30°, 45°, 60°, 75° and 90°) on the flexural characteristics and fracture behaviour of PLA specimens produced using FDM. Specimens that met ISO 178 were printed under constant process conditions and put into three-point bending tests. The findings indicate that the flat orientation (0°) has the best elastic modulus (1808 ± 45 MPa) and flexural strength (47.6 ± 2.2 MPa) which are 15% and 124% better than the configuration at 90°, respectively. The monotonic decrease of elongation at break with the orientation angle and nonmonotonic increase in the mass of the specimen, respectively, before and after 30°. The two trends are also manifested in the specific strength, in which the 0° orientation is the best. The fracture surface morphology is associated with layer-orientated crack propagation at angles that increase to higher angles and then change to through-layer fracture at 0°. The results make a quantitative recommendation for the orientation choice in flexure-critical FDMs.

Keywords: build orientation, fused deposition modelling, flexural properties, PLA, fracture behaviour.

Introduction

Additive manufacturing and, more specifically fused deposition modelling (FDM) has established itself as a multifunctional system of producing polymer parts in the automotive [1], aerospace [2], protective clothing [3], biomedical [4] and consumer industries. The anisotropic microstructure formed by superposition of deposited layers of materials in FDM has the property of a strong dependence of mechanical action on the spatial relationship between deposited filament roads and applied loads [5]. FDM does not restrict the designer to any fixed manufacturing process but instead enables the designer to change the build orientation as a process parameter directly changing the internal architecture and interlayer bond density of the finished part without changing material composition or infill geometry [6-10].

In FDM, a part can call the build orientation the angular position of the part relative to the print bed when it is being fabricated [11]. In cases where the specimen is printed flat (0°) the long axis is parallel to the build plate, and the applied load in bending occurs across many continuous layers of filament; as the angle of orientation goes toward 90 degrees, the specimen changes the geometry to an edge-on geometry, where a smaller number of taller layers cross the cross section. This change in geometry essentially transforms the number of interlayer interfaces that is being crossed by the stress field, the extent of filament continuity with the direction of loading and the useful cross-sectional area of bonded material in opposition to fracture. As a result, the orientation angle has a strong effect on the stiffness [12], strength [13] and failure mode [14].

Other earlier studies have recorded the anisotropic behaviour of FDM-fabricated components in tensile and flexural loads. Research on PLA and ABS has uniformly found flat-printed constructions to have a higher strength in configurations with a load path running parallel to the filament direction, and a vertical structure being the weakest structural connection [15-17]. Studies of raster angle, layer thickness, and infill density have helped to understand more about FDM process-property relationships, but the systematic impact of continuous variation of orientation angle, especially at intermediate angles between 0° and 90°, to flexural response has not been fully characterised [18-20]. The number of discrete orientations that most of the currently existing studies use is only two or three, which restricts the resolution with which transitional mechanical behaviour can be registered.

The gap that the current research will bridge is by determining flexural mechanical and fracture morphology at seven build orientation angles (0° to 90° in 15° steps) with standardised specimens made of commercial PLA filament using a Prusa Mini FDM printer. All other parameters of the process except the orientation were kept constant. Alongside traditional flexural measures, elastic modulus, flexural

strength, and flexural strain at break, specific strength is documented in order to put performance in context with the mass change which occurs due to orientation sensitive printing efficiency.

Materials and methods

Commercially available materials PLA filament (1.75 mm diameter, Prusa Research a.s., Czech Republic) were made into specimens by printing on a Prusa Mini FDM printer with a 0.4 mm brass nozzle and a glass fibre build plate as mentioned in [21; 22]. Before printing, the filament was dried at 40 °C for one hour with an eSUN eBOX Lite drying unit to remove moisture that could be absorbed, thus reducing both the quality of the printed product and the mechanical performance. All printing parameters are summarised in Table 1. The layer thickness of 0.2 mm was chosen as a compromise between structural resolution and printing efficiency. The infill density was held at 40% and the pattern was rectilinear to isolate orientation effect on the other geometric variables.

Table 1

FFF process parameters and printing conditions

Printing Parameter	Value/Description
Filament diameter, mm	1.75
3D printer	Prusa Mini
Nozzle diameter, mm	0.4
Build plate	Glass fibre
Extrusion temperature, °C	215
Bed temperature, °C	60
Print speed, $mm \cdot s^{-1}$	25
Layer thickness, mm	0.2
Shell thickness, mm	0.2
Infill density, %	40
Infill pattern	Rectilinear

There were seven angles of orientation of the buildings studied: 0°, 15°, 30°, 45°, 60°, 75°, and 90°. The short and long edges of the specimen tilt at an angle, θ, which determines the angle of the short and long sides of the specimen versus the bed of the printer, as shown in Fig. 1. When 0 corresponds to the specimen lying flat and when 90 corresponds to the specimen standing on its short end. The intermediate angles obtain increasingly tilted build geometries where the filament deposition pattern crosses the specimen cross-section at different angles. All samples were of ISO 178 geometry (80 × 10 × 4 mm), and the thickness of the sample remained constant at 4 ± 0.1 mm throughout the study. The replica was made on all the angles of orientation angles, producing a total of 35 replicate specimens.

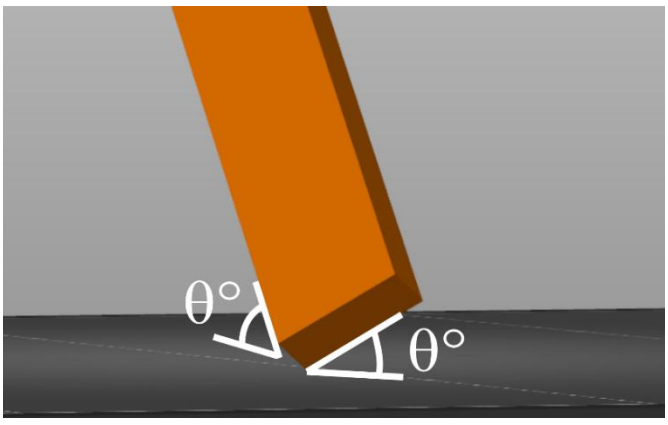

Fig. 1. **Schematic illustration of the build orientation angle θ, inclination of the short and long edges relative to the printer bed**

A Mecmesin Multi-Test 2.5-i universal testing machine (PPT Group UK Ltd., Slinfold, UK) with a 250 N load cell was used to perform flexural testing with a three-point bending configuration at a cross-head speed of 2 mm/min as per ISO 178. The mass of each sample was measured before testing and

recorded using high-precision KERN ABT 5NM analytical balance (resolution 0.000001 g, maximum capacity 100 g) as mentioned in [23-25]. Of every test, elastic modulus, flexural strength and flexural strain at break were obtained. The specific strength was calculated as the ratio of flexural strength to specimen mass and gave a weight-normalised performance measure used in the lightweight design.

Results and discussion

Fig. 2 gives representative flexural stress(σ)-strain(ε) curves at the seven orientation angles. All specimens were characterised by an initial linear elastic regime and a yield transition, which was followed by plastic deformation before failure. The 0° specimen is characterised by a significantly prolonged plastic plateau and the maximum stress, and the specimens that are printed at angles steeper than 30° exhibit steadily steeper post-peak drops and fracture earlier which implies that ductile behaviour decreases with increasing orientation. The mechanical property measurements obtained from these curves are summarised in Table 2.

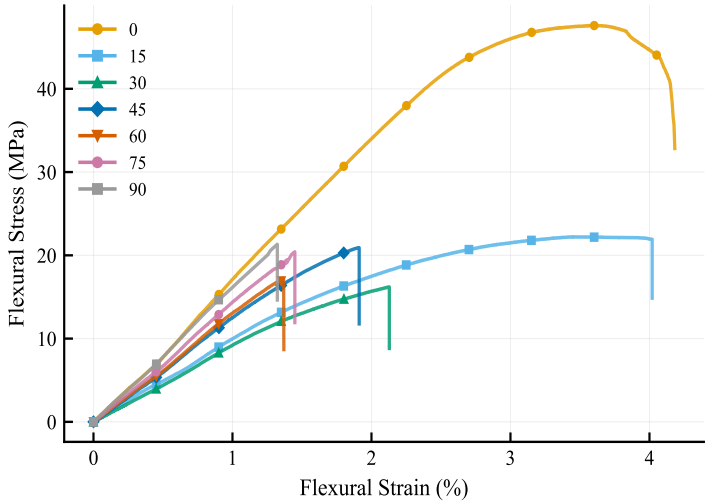

Fig. 2. **Representative flexural stress(σ)-strain(ε) curves for specimens printed at various orientation angles (0°-90°)**

Table 2

Flexural mechanical properties as a function of the orientation angle

Build orientation angle θ	Elastic modulus E, MPa	Flexural strength σ, MPa	Flexural strain at break ε_f, %	Mass m, g	Specific strength, kN·m·kg^{-1}
0°	1808 ± 45	47.6 ± 2.2	4.1 ± 0.16	2.28 ± 0.01	66.3 ± 1.7
15°	978 ± 33	22.2 ± 0.3	4.0 ± 0.07	2.23 ± 0.01	31.9 ± 0.2
30°	916 ± 11	16.2 ± 0.7	2.1 ± 0.06	2.13 ± 0.01	24.0 ± 0.6
45°	1262 ± 48	21.0 ± 0.2	2.0 ± 0.09	2.26 ± 0.01	29.1 ± 0.2
60°	1235 ± 53	17.1 ± 0.3	1.4 ± 0.02	2.32 ± 0.01	23.8 ± 0.2
75°	1387 ± 24	20.4 ± 0.4	1.4 ± 0.04	2.36 ± 0.01	27.4 ± 0.3
90°	1567 ± 42	21.3 ± 0.5	1.3 ± 0.05	2.41 ± 0.01	28.2 ± 0.4

The 0° orientation yielded the best elastic modulus (1808 ± 45 MPa) and flexural strength (47.6 ± 2.2 MPa), which is 15% and 124% higher than the following best configuration (90°, 1567 ± 42 MPa; 21.3 ± 0.5 MPa). This is due to this high performance, where filament roads are maximised in the long axis of the specimen, where maximum bending stress occurs in three-point flexure. When $\theta = 0$, the load acts in tension on the bottom face and in compression on the top face. The inter-road bonding is so dense over the entire cross-section that concentrations of stress are reduced, and initiation of cracks is postponed.

These results are consistent with the broader FDM literature, where flat-printed PLA and ABS specimens have similarly been shown to outperform edge-on and upright configurations under flexural

and tensile loading [15-17]. The partial modulus recovery observed beyond 30° also aligns with laminate analogy models reported for FDM anisotropy [5], where competing interface-density and filament-continuity effects govern stiffness at intermediate angles.

There is a significant nonmonotonic trend in the data of the elastic modulus. The modulus is highest at 0° with a value of 1808 MPa and a low of 916 ± 11 MPa at 30° and finally increases gradually at 45° (1262 ± 48 MPa), 60° (1235 ± 53 MPa) 75° (1387 ± 24 MPa), and 90° (1567 ± 42 MPa). This behaviour corresponds to competing geometric effects: at 15-30°, the filament roads subtend an acute angle with the bending plane which optimises the fraction of weak interlayer interfaces intersected by the stress field. Beyond 30°, the build geometry switches to an edge-on geometry whereby each layer implies a larger bonded cross-sectional area perpendicular to the load, and thus, to some extent restores stiffness. The 90° structure, although with the highest density of the interlayer interface in the beam cross-section, recovers much of the modulus due to the orientation of the layers such that the compressive and tensile zones are in large numbers with intact filament walls parallel to the bending axis. This process agrees with classical laminate theory of FDM-printed structures.

The flexural strength also reduces less in a systematic manner compared with the modulus, with the 0° specimen prevailing. It also shows that the intermediate angles (45°-90°) fall within the range of 17.1-21.3 MPa, with the weakest being 30° (16.2 ± 0.7 MPa). It seems that the 30° orientation is a mechanical minimum, since it just orients interlayer boundaries at an angle that is close to the maximum shear stress plane (45° to the neutral axis), thus, favouring inter-layer shear failure at relatively low applied loads. The elongation at break decreases monotonically from 0° to 1.3 ± 0.05% at 90° indicating a progressive depletion of the ductility due to the progressive loss in the contribution of the deformation mechanisms with increasing θ. The interlayer bond stretching governs the deformation at higher orientation angles and does not accommodate plastic strain as easily as possible.

The mass of the specimen shows a nonmonotonic trend throughout the angular span (Table 2), with a decrease in value between 0° showing a value of 2.28 ± 0.01 g and a minimum of 2.13 ± 0.01 g at 30°, rising to 2.41 ± 0.01 g at 90°, and an increase in mass of ~6% between 0° and 90°. The shape of this V-shaped profile of mass indicates the changes in orientation of the filling pattern of the angled cross-section; at the lowest angles near 30° the rectilinear infill has the lowest efficiency and least material consumption, and at the steeper angles extra perimeter roads must be made to retain the geometry of the outer shell. Although the strength advantage of the 0° configuration is partially reduced by the increase in mass at higher angles, the 0° specimen still achieves the best specific strength (66.3 ± 1.7 $kN \cdot m \cdot kg^{-1}$) being 176 per cent above the weakest configuration (30°, 24.0 ± 0.6 $kN \cdot m \cdot kg^{-1}$). This proves the fact that despite material consumption, the flat orientation offers definitely better weight-normalised flexural performance.

Orientation-dependent failures can be seen in the analysis of fracture surfaces (Fig. 3). Fracture surfaces at 0° are approximately planar and perpendicular to the axis of the specimen, which is in line with tensile failure of filament roads on the tension side of the beam and extension of transversal cracks through the cross section.

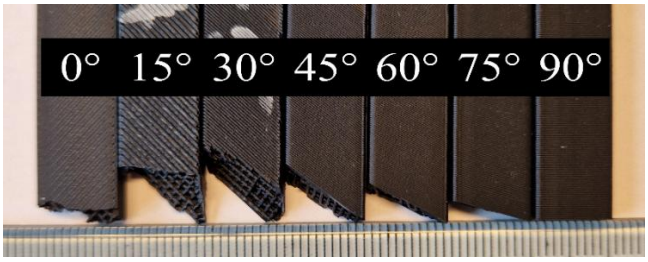

Fig. 3. **Fracture behaviour of the specimens at each orientation angle (scale bar: 1 mm)**

When the angle of orientation increases, the fracture surfaces are inclined and irregular, which means that crack propagation is diverted on the layers. Fracture planes at 30° and 45° are parallel to the printed interface of the layers, and this proves that interlayer bonding controls failure in the mentioned arrangements. Fractures at 75° and 90° are stepped and representative of mixed-mode interlayer and transverse cracking because, due to the vertical layout of the layers, several competing tracks are forced. These data are in agreement with the intermediate modulus recovery observed at greater angles and

allow the conclusion that filament continuity and interface orientation to the applied stress field are the main factors that determine the flexural response in FDM-printed PLA.

Conclusions

1. Seven orientations of the building were tested for their influence on the flexural performance of FDM-printed PLA. High elastic modulus (1808 ± 45 MPa), flexural strength (47.6 ± 2.2 MPa) and specific strength (66.3 ± 1.7 $kN \cdot m \cdot kg^{-1}$) which were 97%, 194%, and 176% greater than the lowest values at 30°.
2. There was a nonmonotonic trend in elastic modulus with the lowest elastic modulus occurring at 30°, and some recovery in elastic modulus up to 90° and mass followed a V-shaped trend.
3. The fracture behaviour changed from through-layer failure at 0° to interlayer delamination at intermediate angles with mixed-mode cracking occurring at 75°-90°. These findings give explicit numerical advice on orientation selection of flexure-critical FDM design.

Author contributions

Conceptualization, H.K.M., and J.V.S.; methodology, H.K.M., A.A. and J.V.S.; software, H.K.M. and V.V.; validation, J.V.S.; formal analysis, H.K.M. and A.A.; investigation, H.K.M., A.A. and V.V.; data curation, H.K.M. and A.A.; writing – original draft preparation, H.K.M.; writing – review and editing, J.V.S; visualization, J.V.S.; project administration, J.V.S.; funding acquisition, H.K.M. All authors have read and agreed to the published version of the manuscript.

References

[1] Vasco J. C. Chapter 16 - Additive manufacturing for the automotive industry, in Handbooks in Advanced Manufacturing, J. Pou, A. Riveiro, and J. P. B. T.-A. M. Davim, Eds. Elsevier, 2021, pp. 505-530. DOI: 10.1016/B978-0-12-818411-0.00010-0

[2] Blakey-Milner B., Gradl P., Snedden G., Brooks M., Pitot J., Lopez E., Leary M., Berto F., du Plessis A. Metal additive manufacturing in aerospace: A review, Mater. Des., vol. 209, 2021, p. 110008, DOI: 10.1016/j.matdes.2021.110008

[3] Vejanand S. R., Janushevskis A., Vaicis I. Analyzing Efficiency of Ventilation Elements Used in Protective Clothing With Simplified Model, Eng. Rural Dev., vol. 23, 2024, pp. 169-177, DOI: 10.22616/ERDev.2024.23.TF036

[4] Kumar R., Kumar M., Chohan J. S. The role of additive manufacturing for biomedical applications: A critical review, J. Manuf. Process., vol. 64, 2021, pp. 828-850, DOI: 10.1016/j.jmapro.2021.02.022

[5] Dixit S., Liu S., Murdoch H. A., Smith P. M. Investigating build orientation-induced mechanical anisotropy in additive manufacturing 316L stainless steel, Mater. Sci. Eng. A, vol. 880, 2023, p. 145308, DOI: 10.1016/j.msea.2023.145308

[6] Papa I., Bruno M., Napolitano F., Esposito L., Lopresto V., Russo P. Numerical modeling and validation of auxetic cell geometries for FDM infill pattern improvement, Prog. Addit. Manuf., vol. 10, no. 9, 2025, pp. 6353-6367, DOI: 10.1007·s-140964-025-00980-2

[7] Garg S., Singh A., Murtaza Q. Measuring the Impact of Infill Pattern and Infill Density on the Properties of 3D-Printed PLA via FDM, J. Mater. Eng. Perform., vol. 34, no. 19, 2025, pp. 22597-22610, DOI: 10.1007·s-111665-025-10837-y

[8] Kumaresan R., Kadirgama K., Samykano M., Harun W. S. W., Thirugnanasambandam A., Kanny K. In-depth study and optimization of process parameters to enhance tensile and compressive strengths of PETG in FDM technology, J. Mater. Res. Technol., vol. 37, 2025, pp. 397-416, DOI: 10.1016/j.jmrt.2025.06.013

[9] Madhuraghava P., Jayachandra Reddy G. Mechanical performance of FDM-printed PLA: a comparative study of single, double and triple infill pattern configurations, World J. Eng., 2025, DOI: 10.1108/WJE-05-2025-0364

[10] Kumaresan R., Kadirgama K., Samykano M., Harun W.S.W., Thirugnanasambandam A., Aslfattahi N., Samylingam L., Kok C.K., Ghazali M.F. Optimization of inter-layer printing parameters for enhanced mechanical performance of PETG in Fused Deposition Modeling (FDM), Results Eng., vol. 25, 2025, p. 104564, DOI: 10.1016/j.rineng.2025.104564

[11] Langelaar M. Combined optimization of part topology, support structure layout and build orientation for additive manufacturing, Struct. Multidiscip. Optim., vol. 57, no. 5, 2018, pp. 1985-2004, DOI: 10.1007·s-100158-017-1877-z
[12] Zamanian M., Mollaei-Alamouti V., Payan M. Directional strength and stiffness characteristics of inherently anisotropic sand: The influence of deposition inclination, Soil Dyn. Earthq. Eng., vol. 137, 2020, p. 106304, DOI: 10.1016/j.soildyn.2020.106304
[13] Yuan H., Dong E., Jia Z., Jia L., Quan S., Ma M., Yang Y., Feng M., Banthia N., Zhang Y. The influence of pore structure and fiber orientation on anisotropic mechanical property of 3D printed ultra-high-performance concrete, Constr. Build. Mater., vol. 471, 2025, p. 140760, DOI: 10.1016/j.conbuildmat.2025.140760
[14] Rahmati A., Nikzad M. H., Heidari-Rarani M., Bagherifard S. Bilinear constitutive model for the anisotropic failure prediction of PLA specimens produced by material extrusion additive manufacturing, Prog. Addit. Manuf., vol. 10, no. 4, 2025, pp. 2089-2104, DOI: 10.1007·s-140964-024-00737-3
[15] Llanos C. M., Saakes D., Mehrpouya M. Additive manufacturing of adaptive architected structures for enhanced protective equipment, Eur. J. Mech. - A·s-1olids, vol. 112, 2025, p. 105649, DOI: 10.1016/j.euromechsol.2025.105649
[16] Qiu S., Liu Z., Wang M., Xu M., Chen Y., Huang T., Tian W. Z-axis 3D-printing performance improvement by modifying polylactic acid composites using microcrystalline cellulose and polybutylene adipate-co-terephthalate, Int. J. Biol. Macromol., vol. 339, 2026, p. 149842, DOI: 10.1016/j.ijbiomac.2025.149842
[17] Tosto C., Saitta L., Blanco I., Fichera G., Evangelista M., Jose J., Pantaleoni A., Bavasso I. Additive Manufacturing of Carbon Fiber Cores for Sandwich Structures: Optimization of Infill Patterns and Fiber Orientation for Improved Impact Resistance, Journal of Manufacturing and Materials Processing, vol. 9, no. 9. p. 299, 2025. DOI: 10.3390/jmmp9090299
[18] Jain J., Kumar N., Taufik M., Jain P. K. Optimum part filling via layer-wise variation of raster angle in fused filament fabrication, Int. J. Interact. Des. Manuf., vol. 19, no. 9, 2025, pp. 6053-6063, DOI: 10.1007·s-112008-024-02189-z
[19] Kaya H., Yaman U. Torsional characteristics of a novel infill pattern in material extrusion type of additive manufacturing: random lines, Prog. Addit. Manuf., vol. 11, no. 1, 2026, pp. 1261-1272, DOI: 10.1007·s-140964-025-01410-z
[20] Guzman-Bautista A., López-Arrabal A., Sanchez-Oro-Aguado E., Fernández-Gorgojo A., García-Galán R., Badesa F.J., Vizan-Idoipe A. Quasi-Uniform Density Non-Solid Infill Strategy for Axisymmetric Non-Planar Additive Manufacturing, Appl. Sci., vol. 15, no. 11, 2025, DOI: 10.3390/app15115899
[21] Sanchaniya J. V, Kannathasan K. R., Vejanand S. R., Joshi J., Lasenko I. Effect of Infill Pattern Design on Tensile Strength of Fused Deposition Modelled Specimens, Environment Technology Resources - Proceedings of the 16th International Scientific and Practical Conference, 2025, vol. 4, pp. 375-382. DOI: 10.17770/etr2025vol4.8409
[22] Sanchaniya J. V, Smogor H., Gobins V., Noël V., Lasenko I., Rackauskas S. Layer-by-Layer Integration of Electrospun Nanofibers in FDM 3D Printing for Hierarchical Composite Fabrication, Polymers (Basel)., vol. 18, no. 1, 2026, DOI: 10.3390/polym18010078
[23] Sanchaniya J. V Comparative Analysis of Thermal Characteristics: Virgin Polyacrylonitrile (PAN) versus Electrospun PAN Nanofibre Mats, Latv. J. Phys. Tech. Sci., vol. 61, no. 4, 2024, pp. 98-105, DOI: 10.2478/lpts-2024-0031
[24] Sanchaniya J.V., Lasenko I., Vijayan V., Smogor H., Gobins V., Kobeissi A., Goljandin D. A Novel Method to Enhance the Mechanical Properties of Polyacrylonitrile Nanofiber Mats: An Experimental and Numerical Investigation, Polymers (Basel)., vol. 16, no. 7, 2024, p. 992, DOI: 10.3390/polym16070992
[25] Sanchaniya J.V., Lasenko I., Kanukuntla S.P., Smogor H., Viluma-Gudmona A., Krasnikovs A., Tipans I., Gobins V. Mechanical and Thermal Characterization of Annealed Oriented PAN Nanofibers, Polymers (Basel)., vol. 15, no. 15, 2023, DOI: 10.3390/polym15153287